Taylor & Francis
Taylor & Francis Group

Vehicle System Dynamics
International Journal of Vehicle Mechanics and Mobility

ISSN: (Print) (Online) Journal homepage: https://www.tandfonline.com/loi/nvsd20

Improved accuracy for FASTSIM using one or three flexibility values

Edwin Vollebregt & Petr Voltr

To cite this article: Edwin Vollebregt & Petr Voltr (2022): Improved accuracy for FASTSIM using one or three flexibility values, Vehicle System Dynamics, DOI: 10.1080/00423114.2022.2042331

To link to this article: https://doi.org/10.1080/00423114.2022.2042331

© 2022 The Author(s). Published by Informa UK Limited, trading as Taylor & Francis Group

Published online: 01 Mar 2022.

Submit your article to this journal

Article views: 246

View related articles

View Crossmark data

Full Terms & Conditions of access and use can be found at
https://www.tandfonline.com/action/journalInformation?journalCode=nvsd20

VEHICLE SYSTEM DYNAMICS
https://doi.org/10.1080/00423114.2022.2042331

RESEARCH ARTICLE

OPEN ACCESS Check for updates

Improved accuracy for FASTSIM using one or three flexibility values

Edwin Vollebregt [a] and Petr Voltr [b]

[a]Vtech CMCC, Rotterdam, The Netherlands; [b]University of Pardubice, Pardubice, Czech Republic

ABSTRACT

This paper presents a correction and an extension of the FASTSIM approach for the computation of the wheel–rail creep forces. The correction concerns the variants of FASTSIM using a single flexibility value. Kalker's formula for this gives up to 41% too large flexibility in situations with mixed creepage, underestimating the creep forces by 29%. This is corrected using new approaches for the flexibilities' combination. The extension concerns the variants of FASTSIM using three flexibility values. These variants misrepresent the creep force direction at large creepage. This is resolved using a blending approach, that roughly halves the errors of FASTSIM compared to CONTACT.

ARTICLE HISTORY
Received 18 October 2021
Revised 11 January 2022
Accepted 5 February 2022

KEYWORDS
Rail-wheel interaction; creep forces; friction; vehicle-track interaction

1. Introduction

The simulation of rail vehicle–track interaction requires the fast approximate calculation of the wheel–rail creep forces [1]. The main algorithms used in vehicle dynamics today are Polach's algorithm [2,3], the easiest to use, table-based approaches such as USETAB [4], the closest to CONTACT, and FASTSIM [5–8], the most flexible and extendable beyond basic elliptical contacts.

Multiple variants of FASTSIM have been proposed, with different choices for the discretization strategy (FASTSIM versus FASTSIM2) and discretization grid (constant or variable step sizes), elliptical or parabolic traction bounds, and the choice of the flexibility parameter, using one or three flexibility values [7]. Three flexibilities L_i were proposed by Kalker [5,6][1]:

$$L_\xi = \frac{8a}{3C_{xx}G}, \quad L_\eta = \frac{8a}{3C_{yy}G}, \quad L_\phi = \frac{\pi a\sqrt{a/b}}{4C_{yz}G}. \tag{1}$$

They align FASTSIM with the linear theory for pure longitudinal, pure lateral, or pure spin creepage. Further, Kalker defined a weighting approach to combine three flexibilities into a single value

$$L = L_{orig} = \frac{|\xi|L_\xi + |\eta|L_\eta + \sqrt{ab}|\phi|L_\phi}{\sqrt{\xi^2 + \eta^2 + ab\phi^2}}. \tag{2}$$

CONTACT Edwin Vollebregt edwin.vollebregt@cmcc.nl

© 2022 The Author(s). Published by Informa UK Limited, trading as Taylor & Francis Group
This is an Open Access article distributed under the terms of the Creative Commons Attribution-NonCommercial-NoDerivatives License (http://creativecommons.org/licenses/by-nc-nd/4.0/), which permits non-commercial re-use, distribution, and reproduction in any medium, provided the original work is properly cited, and is not altered, transformed, or built upon in any way.

Upon detailed consideration, we identified a shortcoming in this Equation (2). The formula looks like the weighted mean of flexibilities L_i with weights $|\xi|, |\eta|$ and $\sqrt{ab}|\phi|$. However, the weights are squared in the denominator instead of being summed directly. This produces unwanted results in cases of mixed creepage. A particular example considers a contact ellipse with equal flexibilities $L_\xi = L_\eta$ ($a/b \approx 3$), with equal $\xi = \eta$ and with no spin creepage. In this case, the actual outcome is $\sqrt{2}$ times higher than the desired result $L = L_\xi = L_\eta$. In absense of slip, this reduces the forces F_x, F_y computed by FASTSIM by a factor $\sqrt{2}$, producing errors of 29%.

In this technical note, we consider the flexibility values that are used in FASTSIM. We propose new ways for their combination, improving the agreement between CONTACT and FASTSIM using a single flexibility value. Then we proceed with a shortcoming of the approach using three flexibility values. We propose a new blending approach, that roughly halves the errors in the wheel–rail creep forces obtained from FASTSIM, compared to CONTACT.

2. Improvement of FASTSIM with 1 flexibility

Various formulas can be used as alternatives to Equation (2). Two straightforward ideas are to use weighted means with weights that are linear or quadratic in creepages ξ, η, ϕ:

$$L_{lin} = \frac{|\xi| L_\xi + |\eta| L_\eta + \sqrt{ab}|\phi| L_\phi}{|\xi| + |\eta| + \sqrt{ab}|\phi|}, \tag{3}$$

$$L_{sqr} = \frac{\xi^2 L_\xi + \eta^2 L_\eta + ab\phi^2 L_\eta}{\xi^2 + \eta^2 + ab\phi^2}. \tag{4}$$

As CONTACT and FASTSIM are based on different elasticity models, different patterns are obtained for the surface tractions. This is illustrated in Figure 1 for a basic testcase, a circular contact with small creepage $\xi = \eta = -0.001, \mu = 0.3, m_x = 81, m_y = 45$, showing the surface tractions p_x, p_y along the centreline $y = 0$. Even though different spatial patterns are found for the tractions p_x, p_y, the resultant forces may be balanced using the right flexibility values. For the longitudinal force, this is achieved using $L = L_\xi = 0.647$ from Equation (1). This gives higher tractions for CONTACT at some places (blue shaded region) cancelled by lower tractions at other places (red shaded region).

The right part of Figure 1 shows slightly lower lateral tractions p_y for CONTACT than the corresponding longitudinal p_x in the left part of the figure. This calls for a different flexibility value, $L = L_\eta = 0.727$, in order to match the resultant $F_y^{cntc} = 0.00370$. The purpose of weighting is to strike a balance between these different demands. The dashed lines in Figure 1 show the results for the combined flexibility value of Equation (2). This takes the mean value 0.687 multiplied by $\sqrt{2}$, resulting in $L = L_{orig} = 0.971$. This increased flexibility reduces the tractions and resultant forces.

The best value for the flexibility L is the one that gives the best compromise for the different locations, and for the forces F_x and F_y. It appears possible to obtain such a value by minimising the difference to the linear theoretic forces:

$$L_{nrm} = \text{argmin}_L \|\mathbf{F}^{fsim} - \mathbf{F}^{lin}\|^2 = \text{argmin}_L \left\{ \left(F_x^{fsim} - F_x^{lin}\right)^2 + \left(F_y^{fsim} - F_y^{lin}\right)^2 \right\} \tag{5}$$

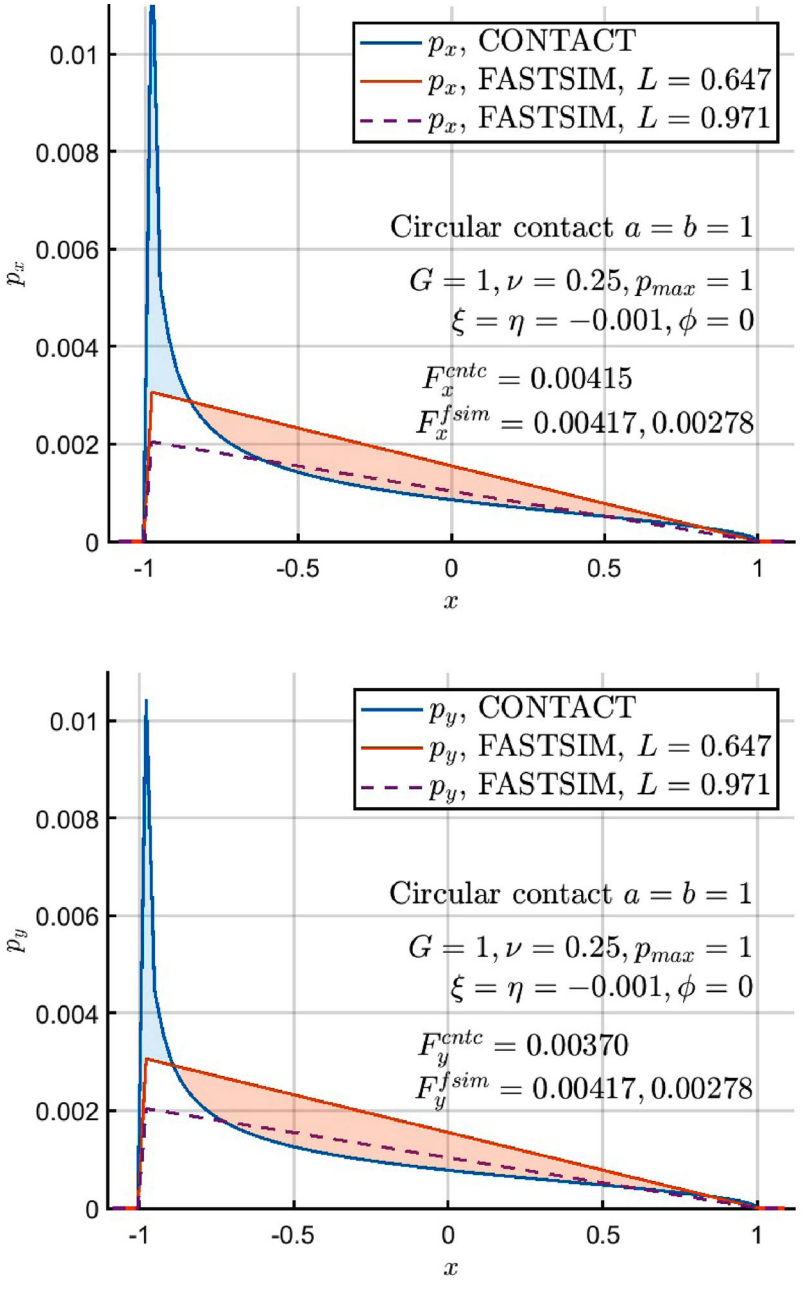

Figure 1. Surface tractions along centreline $y = 0$ (left: p_x, right: p_y) computed by CONTACT for a circular contact with small creepage, and corresponding results for FASTSIM using a single flexibility value.

Kalker presented the forces obtained from FASTSIM in situations of full adhesion [6, § 3.7.1][2]. Inserting these in Equation (5) we get

$$\min_L \left\{ \left(\frac{8a^2b}{3L}\xi - abGC_{xx}\xi \right)^2 + \left(\frac{8a^2b}{3L}\eta + \frac{\pi a^3 b}{4L}\phi - abGC_{yy}\eta - (ab)^{3/2}GC_{yz}\phi \right)^2 \right\} \tag{6a}$$

$$\div ab, \quad K := \frac{1}{L}, \quad f_3 := \frac{8a}{3}, \quad f_4 := \frac{\pi a^2}{4}, \quad c := \sqrt{ab}$$

$$= \min_K \left\{ \left(f_3 K\xi - GC_{xx}\xi\right)^2 + \left(f_3 K\eta + f_4 K\phi - GC_{yy}\eta - cGC_{yz}\phi\right)^2 \right\} \tag{6b}$$

Taking the derivative with respect to K and setting to zero we find

$$L_{nrm} = \frac{\left(f_3\xi\right)^2 + \left(f_3\eta + f_4\phi\right)^2}{f_3 GC_{xx}\xi^2 + \left(f_3\eta + f_4\phi\right) \cdot \left(GC_{yy}\eta + cGC_{yz}\phi\right)}. \tag{7}$$

A difference with formulas (3) and (4) is that creepages η and ϕ are not used separately anymore, but appear now in specific linear combinations. An interpretation for this is that there exists an 'effective lateral stiffness' that varies with the proportion of creepages η and ϕ (and with contact patch size, shape, and materials used). Certain creepages η, ϕ that would produce considerable lateral force by themselves may result in $F_y = 0$ if taken together, such that there's apparently no stiffness associated with that combination. For FASTSIM, this happens at $\phi = -\eta f_3/f_4$, for the linear theory at $\phi = -\eta C_{yy}/cC_{yz}$.

The ratios $f_3/f_4 = 32/\pi a$ and C_{yy}/cC_{yz} are generally different, such that the two factors in the denominator of (7) cross zero at different combinations of η and ϕ. As a result, we may find negative values for L at specific creep combinations. This is justified by our objective, to match the forces obtained from FASTSIM to those of CONTACT. If CONTACT and FASTSIM think differently about the direction of the net lateral force, then a negative stiffness is permitted to change the force direction in FASTSIM.

Equation (7) yields infinite flexibility when $\xi = 0, \phi/\eta = -C_{yy}/cC_{yz}$. This produces zero tractions in FASTSIM, $F_x = F_y = 0$. This result is desired for small creepage where the linear theory gives a good approximation, but may be off at larger creepage. A similar reasoning applies to zero flexibility $L_{nrm} = 0$, obtained when $\xi = 0, \phi/\eta = -f_3/f_4$. This concerns situations where FASTSIM produces $F_y = 0$ whereas the linear theory gives a nonzero value. In this case, a precise zero must be replaced by a small value to prevent division by zero when L is used in FASTSIM.

Equation (7) is simplfied by omitting the lateral–spin interactions, setting cross terms $\eta\phi = 0$. This yields one further proposal:

$$\frac{1}{L}_{nrm} \approx \frac{f_3 GC_{xx}\xi^2 + f_3 GC_{yy}\eta^2 + f_4 cGC_{yz}\phi^2}{\left(f_3\xi\right)^2 + \left(f_3\eta\right)^2 + \left(f_4\phi\right)^2}$$

$$\rightarrow \frac{1}{L_{crss}} = \frac{1}{\xi^2 + \eta^2 + (\phi f_4/f_3)^2} \cdot \left(\frac{\xi^2}{L_\xi} + \frac{\eta^2}{L_\eta} + \frac{(\phi f_4/f_3)^2}{L_\phi} \right) \tag{8}$$

Avoiding the zeros for the effective lateral stiffness, this L_{crss} is easier to use than L_{nrm}, and is justified better at larger creepage.

3. Statistical evaluation

The performance of the new methods relative to CONTACT is evaluated using the statistical approach presented in [7,9]. This uses a test-set of 3,220 combinations of contact patch ellipticities a/b and creepage values, that cover the range of parameter values for realistic vehicles and tracks in VSD simulations.

Table 1. Statistics of the errors in total forces F_x and F_y computed by FASTSIM2 using a 640 × 640 grid compared to those computed by CONTACT.

	Errors in F_x			Errors in F_y			
	80%	95%	rms	80%	95%	rms	
Using parabolic traction bound:							
1 flexibility, old weighing L_{orig} (2)	.035	.123	.047	.071	.133	.058	
1 flexibility, new weighing L_{lin} (3)	.016	.044	.019	.034	.088	.037	
1 flexibility, new weighing L_{sqr} (4)	.018	.047	.019	.034	.085	.037	
1 flexibility, new weighing L_{nrm} (7)	.017	.047	.019	.027	.074	.033	←
1 flexibility, new weighing L_{crss} (8)	.015	.046	.019	.034	.078	.034	
3 flexibilities	.027	.061	.026	.054	.087	.041	
Bottom half of creep magnitudes:							
1 flexibility, new weighing L_{nrm} (7)	.030	.059	.025	.050	.089	.045	
3 flexibilities	.023	.039	.019	.051	.085	.039	←
Top half of creep magnitudes:							
1 flexibility, new weighing L_{nrm} (7)	.005	.023	.010	.008	.026	.013	←
3 flexibilities	.037	.076	.031	.056	.090	.042	

Results for CONTACT are computed on grids of 160 × 160 elements, enabled by the new solver GDsteady implemented in CONTACT version 21.1. Results for FASTSIM2 are computed using a grid of 640 × 640 elements, with virtually no error due to the grid discretization.

Figure 2 shows the accuracy of FASTSIM2 compared to CONTACT. The figure displays the statistical distribution of errors $|F_\tau^{fsim} - F_\tau^{cntc}|$, with $\tau = x$ and $\tau = y$. The forces F_x, F_y are the total tangential forces relative to the Coulomb maximum μF_n, with values in the range $[-1, 1]$. The errors in the figure are absolute errors. Percentual differences would show a similar behaviour; in most cases, an absolute difference of 0.1 corresponds roughly to a relative difference of 20% [9]. Key statistics of the distributions are shown in Table 1.

Our test results confirm the shortcoming identified for Equation (2). When using a single flexibility, the results of FASTSIM2 are improved considerably using $L_{lin}, L_{sqr}, L_{nrm}$ or L_{crss} of Equations (3), (4), (7), (8) instead of the original L_{orig} of Equation (2). The same holds for the original FASTSIM algorithm [5] that produces the same results as FASTSIM2 except for the errors due to grid discretization.

A second conclusion is obtained from these results that may be surprising, and that turns around our earlier finding from [7]. With the new formulas, we find that FASTSIM with a single flexibility performs better (on average) than FASTSIM with three flexibilities L_ξ, L_η, L_ϕ according to Equation (1). This is particularly so for cases with large creepage (Table 1, top half of creep magnitudes), where the force direction is governed more by the creepages ξ, η than the stiffnesses L_ξ, L_η.

4. Improvement of FASTSIM with 3 flexibilities

The results of the previous section yield further insight in the behaviour of the contact forces. Rolling contacts behave anisotropically at small creepage, producing different forces $F_x \neq F_y$ for equal creepages $\xi = \eta$. Contact patches that are elongated in rolling direction ($a/b > 3$) have Kalker coefficients $C_{xx} < C_{yy}$ such that $F_x < F_y$, whereas $F_x > F_y$ for shorter and wider contact patches. More isotropic behaviour is found at larger creepage, with $F_x/F_y \approx \xi/\eta$, because tractions and slip take opposite directions.

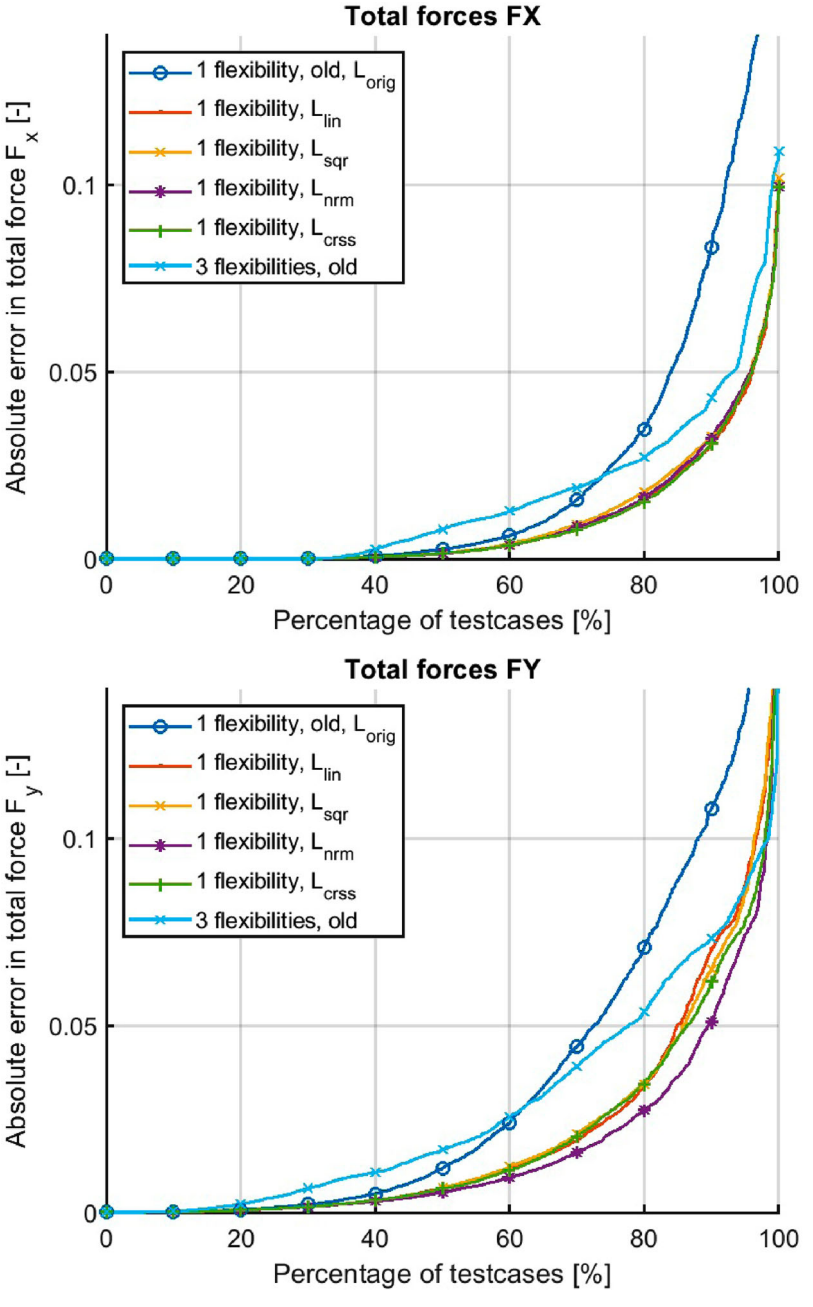

Figure 2. Accuracy of the relative total forces F_x (left) and F_y (right) computed with the FASTSIM2 algorithm on a fine grid w.r.t. CONTACT results.

Considering Equation (1), we see that the three flexibilities are tuned to reflect the anisotropic behaviour at small creepage, introducing errors at larger creepage and larger creep forces. An improvement is obtained using a blending approach, gradually shifting from three separate creepages to a single combined one as total creepage gets larger. This

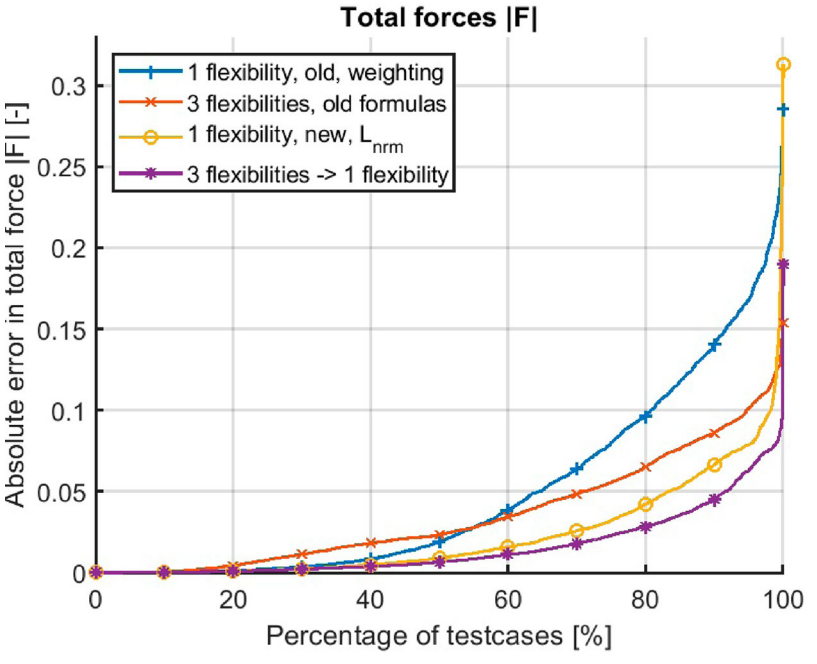

Figure 3. Accuracy of the total force $\|\mathbf{F}\|$ computed with the FASTSIM2 algorithm on a fine grid w.r.t. CONTACT results.

is implemented using three 'characteristic creepages'

$$\xi_{char} = \frac{\mu F_n}{c^2 G C_{xx}}, \quad \eta_{char} = \frac{\mu F_n}{c^2 G C_{yy}}, \quad \phi_{char} = \frac{\mu F_n}{c^3 G C_{yz}}. \tag{9}$$

These are defined as the creepage values for which the forces in linear theory reach the Coulomb maximum value.

The characteristic creepages are used to combine the creepages into a normalised size, f, from which the weight $\bar{f}$ is computed:

$$f = \sqrt{\frac{\xi^2 + \eta^2 + \phi^2}{\xi_{char}^2 + \eta_{char}^2 + \phi_{char}^2}}, \tag{10a}$$

$$\bar{f} = \min\left(1, \max\left(0, \frac{f - f_0}{f_1 - f_0}\right)\right), \tag{10b}$$

$$L_i' = (1 - \bar{f}) L_i + \bar{f} L_{crss}. \tag{10c}$$

The weight $\bar{f}$ is zero for $f \leq f_0$, increasing to one at $f \geq f_1$. Using calibration, we found appropriate settings $f_0 = 0, f_1 = 3$. Using this, three flexibilities perform better again than a single flexibility L_{nrm}, as shown in Figure 3 and Table 2.

5. Conclusions

When using FASTSIM with a single flexibility, there's a mistake in Kalker's original equation for the combined flexibility value. This original formula produces too large

Table 2. Statistics of the errors in total forces F_x and F_y computed by FASTSIM2 using a 640 × 640 grid compared to those computed by CONTACT.

	Errors in $\|\|\mathbf{F}\|\|$			
	80%	95%	rms	
Using parabolic traction bound:				
1 flexibility, old weighing L_{orig} (2)	.096	.168	.075	
3 flexibilities, (1)	.065	.101	.048	
1 flexibility, new weighing L_{nrm} (7)	.042	.079	.038	
blending 3 flexibilities → 1 flexibility (10a)	.029	.063	.026	←

flexibility values and too low contact forces in all situations with mixed creepage. This is repaired using weighted averaging properly or using a minimisation approach. This strongly improves the accuracy of this variant of FASTSIM compared to CONTACT.

When using FASTSIM with three flexibilities, there is an unwanted effect at larger creep values. The flexibilities are fitted on the linear theory, producing anisotropy of the creep forces. In reality, rolling contacts behave more isotropically at large creepage, such that three flexibilities then misrepresent the creep force direction. A blending approach is proposed that automatically switches from three to one flexibilities with increasing creepage. This new blending approach outperforms all the other variants considered in the agreement to CONTACT, roughly halving the error compared to previous versions of FASTSIM.

Notes

1. Kalker used L_i, C_{ij} with numeric subscripts $i, j = 1$–3: easier in sentences and regarding summation, less informative on the physical meaning.
2. Kalker's equation (3.51) has a slight error in the spin term. This should be $\pi a^3 b\phi/(4L_\phi)$ instead of using $a^2 b$.

Disclosure statement

No potential conflict of interest was reported by the author(s).

ORCID

Edwin Vollebregt http://orcid.org/0000-0003-2752-1589
Petr Voltr http://orcid.org/0000-0001-7516-1069

References

[1] Vollebregt EAH, Six K, Polach O. Challenges and progress in the understanding and modelling of the wheel–rail creep forces. Veh Syst Dyn. 2021;59(7):1026–1068.
[2] Polach O. A fast wheel-rail forces calculation computer code. Veh Syst Dyn Suppl. 1999;33:728–739.
[3] Polach O. Creep forces in simulations of traction vehicles running on adhesion limit. Wear. 2005;258:992–1000.
[4] Kalker JJ. Book of tables for the Hertzian creep-force law. In Zobory I, editor. Proceedings of the 2nd Mini Conference on Contact Mechanics and Wear of Wheel/Rail Systems. Hungary: Technical University of Budapest; 1996. p. 11–20.

[5] Kalker JJ. A fast algorithm for the simplified theory of rolling contact. Veh Syst Dyn. 2007;11:1–13.
[6] Kalker JJ. Three-dimensional elastic bodies in rolling contact. Dordrecht, Netherlands: Kluwer Academic Publishers; 1990. (Solid Mechanics and its Applications; vol. 2).
[7] Vollebregt EAH, Wilders P. FASTSIM2: a second order accurate frictional rolling contact algorithm. Comput Mech. 2011;47(1):105–116.
[8] Spiryagin M, Polach O, Cole C. Creep force modelling for rail traction vehicles based on the Fastsim algorithm. Veh Syst Dyn. 2013;51:1765–1783.
[9] Vollebregt EAH, Iwnicki SD, Xie G, et al. Assessing the accuracy of different simplified frictional rolling contact algorithms. Veh Syst Dyn. 2012;50(1):1–17.